



Dynamic energy, exergy and market modeling of a High Temperature Heat and Power Storage System



A. Arabkoohsar^{*}, G.B. Andresen

Department of Engineering, Aarhus University, 8000 Aarhus, Denmark

ARTICLE INFO

Article history:

Received 29 November 2016

Received in revised form

3 March 2017

Accepted 15 March 2017

Keywords:

Smart energy
Dynamic modeling
Energy storage
District heating
Wind energy
Energy market

ABSTRACT

A novel energy storage system that produces both electricity and heat at high efficiencies and takes advantage of a high temperature hot rock cavern thermal energy storage was recently introduced and designed. This study aims at evaluating the performance of the system in terms of energy and exergy efficiencies under realistic operational conditions where the storage supports a number of wind turbines over a long period. The potential value creation of the energy storage system in the local electricity and heat markets is also assessed. The Western part of Denmark with its high number of wind turbine plants and flexible electricity and heat markets have been chosen for the case study of this work. Having both forecasted and realized wind power generation as well as energy prices for the recent years, the system is designed with rigor and a smart bid strategy for the power plant equipped with the energy storage unit for day-ahead and intra-day markets is determined. The results show that the system is able to compensate the fluctuations of wind power plants, and present high annual overall energy and electricity efficiencies of 80.2% and 31.4% and exergy efficiency of 56.1%.

© 2017 Elsevier Ltd. All rights reserved.

1. Introduction

The wind-solar-biomass mix in the electricity and heat sectors is a corner stone in the planned Danish transition to CO₂ neutral energy production by 2035 [1]. However, serious problems must be addressed for the mix to be successful. Some of these are the topic of the recent report “Smart Energy - hovedrapport” by the Danish TSO (Transmission System Operator) Energinet.dk. Here, special attention is brought to flexible demand and the large and costly need for peak production units for the relatively few hours where wind and solar generations are low while the demand remains high. As a consequence, it is estimated that the total socio-economical value of flexible electricity demand in Denmark will increase from current (low) values to about 100 million Euro per year by 2035. The report points out that increased coupling between the energy sectors, i.e. the smart energy concept [2], is the most cost effective instrument to realize the required flexibility. To this end, several well-understood technologies are explored. Most noticeably these include heat pumps, electric boilers and electrical vehicles.

In the present paper, a new innovative utility scale energy conversion and production technology that directly addresses the shortcomings of the current smart energy technologies mentioned above is studied. To this end, the relevant case of an integrated electricity and heating system of Aarhus city embedded in the electricity grid of Western Denmark has been selected. The new technology is a HTHPSS (High Temperature Heat and Power Storage System) that have been designed specifically to accommodate the increased amounts of variable power generation from VRES (Variable Renewable Energy Sources). The defining features of the storage solution is a very high energy efficiency, low-cost for large-scale installations, environmental friendliness, and the ability to support both power and district heating grids at time scales ranging from sub-seconds (primary reserve) to several days, thus allowing e.g. energy trading, forecast error hedging and peak load support. In addition, it does not require special geological features such as those pumped hydro and CAES (compressed air energy storage) do. The study presented here, includes a dynamic market simulation that allows realistic energy and exergy efficiencies as well as electricity and heat market values to be assessed.

The novelty of the paper lies in the detailed assessment of the new smart energy technology HTHPSS that addresses the typical shortcomings of previously explored technologies, in particular, the need of economically attractive up-wards reserve capacity in the

^{*} Corresponding author.

E-mail address: mani.koohsar@yahoo.com (A. Arabkoohsar).

power market. Traditional electricity to heat conversion technologies, such as boilers and heat pumps, can only provide this service by reducing their load on the system whereas HTHPSS can actively produce power from stored heat in a way similar to that of CSP (concentrated solar power).

1.1. Wind energy and energy storage

The fast increase in energy demand along with environmental awareness over the recent years has speeded up the development of renewable energy resource energy production systems in the global scenario [3]. Among all type of renewable energy resources, wind power has emerged as the biggest source in the world with a large technical and economic potential to provide renewable energy. However, wind power is inherently intermittent and hence, it causes power fluctuation issues and challenge for grid stability. Energy storage provides a direct solution to stabilize the power output of the wind turbine (and other unstable power production units). In fact, energy storage can guarantee offsetting the supplied energy fluctuations and energy availability at the time of peak demand, failure in the system or low energy quality in the grid [4]. These are all why considerable attention is being paid to find efficient ways of storing energy to achieve maximum utilization. As a result of these efforts, various storage technologies have emerged so far [5]. These technologies may be classified as mechanical, thermal and electrochemical energy storage systems. The use of battery (electrochemical), as the most widely used type of storage system, is very expensive and not practical for large energy quantities [6]. By far, pumped hydro and compressed air energy storage have been the only suitable systems for large-scale energy storage applications, though each of these systems has its own drawbacks, i.e. huge capital cost and dependence on topographical conditions for pumped hydro [7] and, special geological site need and not fully developed knowledge for compressed air energy storage system [8]. In a recent study, Arabkoohsar and Andresen [9] introduced HTHPSS for large-scale applications, capable of producing both heat and electricity in high efficiency. Fig. 1 illustrates the schematic of this system. The system is most appropriate for the locations with both heat and electricity demand.

As seen in the figure, there is a thermal energy storage system (hot rock cavern with air as intermediate fluid) initially charged to a temperature of 900 K by electrical coils supported by e.g. surplus power produced by wind turbines. Hereafter, the system may be subject to charging or discharging processes. In charging process, surplus power is applied for heating the cavern up to a maximum temperature of 950 K. In discharging steps, the turbine set starts workings and actuates the multistage compressor set as well as the electricity generator. The intake air by the compressors first passes

through intercooler heat exchangers to cool the compressed air down and provide hot water for district heating purposes. Then, it is warmed up before each stage of expansion through heating heat exchangers supported by hot air coming out from the hot storage cavern. Note that this system has been designed with rigor and comprehensive information about this system and its operational details may be found in Ref. [9].

In this work, the performance of HTHPSS is assessed in terms of energy, exergy and economic performance under dynamic practical input energy, energy demand and power and heat prices. For this objective, a comprehensive mathematical model of the system is presented; the system is designed considering the dynamic operational conditions and a smart strategy for bidding in the electricity markets of the host wind turbine farm as well as the local heat market. The schematic of the combined wind turbine and storage system configuration is given in Fig. 2. According to the figure, the

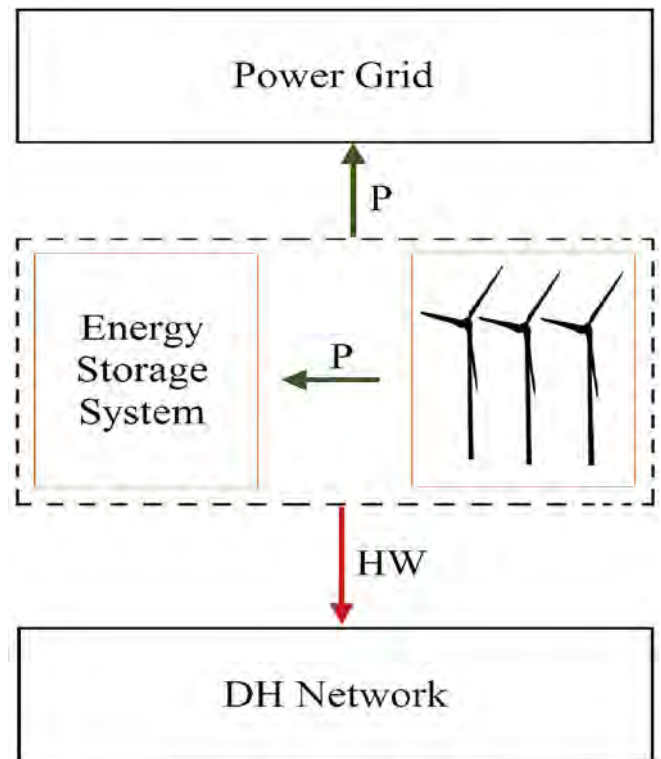


Fig. 2. Schematic drawing of the studied system configuration; DH: district heating, HW: hot water.

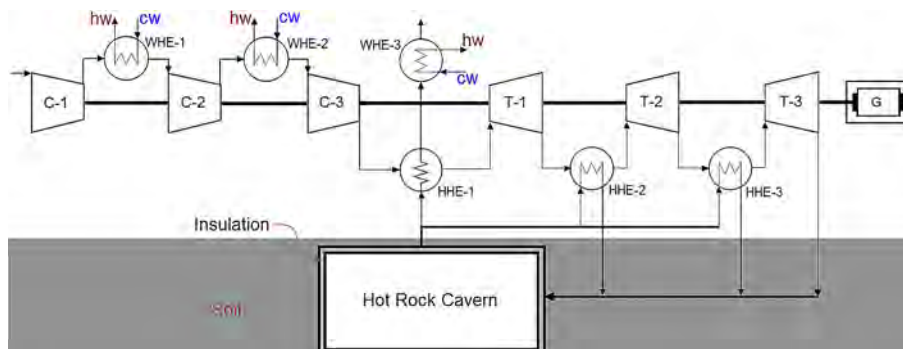


Fig. 1. Schematic of the proposed energy storage system; C: compressor, WHE: water heat exchanger, HHE: heating heat exchanger, T: Turbine, G: electricity generator, cw: cold water, hw: how water.

HTHPSS is charged by supplied power from the wind turbines in low demand period and it supports both the district heating network and the electricity grid in discharging mode, e.g. during peak demand time.

It is worth mentioning that practical information about the wind power production, i.e. hourly electricity and hourly heat prices and weather data of West Denmark, are taken into account as the case study of this work.

1.2. Energy markets

In Denmark, and many other countries, energy producers must bid for their vendible electricity of the next day before 12 a.m. This market is called the day-ahead market and production forecast systems play a key role in determining the value that producers decide to bid at, especially for renewable energy sources [10]. To ensure security of supply it is very important that the producers bid on values that are practically producible, and to incentivize this behavior there are penalties for them if they cannot deliver as promised [11]. As a consequence, producers usually bid based on lower values than the predicted values [12]. In order to make an exact match between the produced power and electricity demand, there are also two more electricity markets, namely, intra-day and intra-hour markets. These markets are closer to the actual hour of production when the accuracy of forecast is much higher, and allow producers to trade their expected imbalances with each other. If any imbalance remains during real-time operation, these are offset by ancillary services at higher prices [13]. Day-ahead prices are given in hourly format and the value depends on the amounts of producible electricity and demand in each hour so that during hours with low demand and high production potential, prices are typically low and, in contrast, prices are high when production and demand are respectively in low and high levels [14]. Thus, the energy production station that takes advantage of an efficient energy storage system can gain higher economic benefits by storing surplus energy during low production price periods and reclaiming this energy during high production price periods. In addition, such a system can avoid penalties in connection with offenses from promised values in day-ahead market.

2. Methodology

In this section, a detailed mathematical description of the energy and exergy analysis as well as economic market value estimates of the energy storage system is presented. The main objective is evaluating the performance of the system under dynamic operational conditions. Generally, the first law efficiency shows how well energy is converted while the second law efficiency can be helpful to evaluate the system performance more accurately, indicating how well availability is used.

2.1. Energy analysis

In the charging phase, the cavern is the only component in operation. It is heated up by using electrical coils that pass through the cavern. In this way, the electrical energy is converted to heat at near 100% efficiency and is efficiently transferred to the air within the cavern. As the air temperature varies, it starts circulating through the cavern and heat is transferred to the rocks as well. To model the heat transfer between the rocks and the hot air within the cavern, based on the energy conservation law, one could write [15]:

$$\rho_r c_r (1 - \varepsilon) \frac{dT_r}{dt} = h_v (T_a - T_r) + \bar{k} \frac{d^2 T_r}{dx^2} \quad (1)$$

$$\rho_a c_{p,a} (1 - \varepsilon) \frac{dT_a}{dt} = h_v (T_r - T_a) - \frac{\dot{\Psi} c_{p,a}}{A} \frac{dT_a}{dx} - \frac{D\pi U}{A} (T_a - T_s) \quad (2)$$

where, ρ , c , T and \dot{m} refer respectively to density, specific heat, temperature and mass flow rate whereas the subscripts r , a and s represent rocks, air and surrounding soil around the cavern, respectively. ε , A and D are the hot rock cavern porosity, its cross sectional area and its diameter, respectively. h_v , \bar{k} and U are volumetric heat transfer coefficient, effective conductivity of the rocks and the overall heat transfer coefficient. These are given by the following three equations, respectively [15]:

$$h_v = 700 \left[\frac{\dot{m}}{Ad} \right]^{0.76} \quad (3)$$

$$\bar{k} = k_r (1 - \varepsilon) + k_a \varepsilon \quad (4)$$

$$U = \left[\frac{1}{h_{in}} + \frac{R}{k_{ins}} \ln \left(\frac{R + \delta_{ins}}{R} \right) + \frac{R}{k_r} \ln \left(\frac{R + \delta_{ins} + \bar{R}}{R + \delta_{ins}} \right) \right]^{-1} \quad (5)$$

where, d , k , h , δ and R are the equivalent diameter of cavern, heat conductivity coefficient, heat convection coefficient, the thickness and radius, respectively. The subscripts in and ins refer to the internal wall of the cavern and insulation. The parameter \bar{R} is the thermal influential distance in the cavern. The rate of heat losses from the cavern (\dot{E}_l) could be calculated as follow:

$$\dot{E}_l = \left[\frac{2k_{ins}\pi L}{\ln \left(\frac{R + \delta_{ins}}{R} \right)} + \frac{2k_{ins}\pi R^2}{\delta_{ins}} \right] (T_{tes} - T_s) \quad (6)$$

Where, L is the height of the cylindrical cavern. Note that for the sake of simplification, the cavern is considered as a vertical cylinder with airflow in only one direction (axial flow) and radial flow is neglected in simulations. Also, the rocks are considered as uniform particles with very small Biot numbers and pressure and viscous terms are neglected. The air properties, which strongly depend on temperature, are extracted from EES [16], whereas the rocks properties were considered to be constants.

In the discharging phase, the first operating component of the system is the compressors set. The total work of compressors set (\dot{W}_C) is calculated as [17]:

$$\dot{W}_C = \sum_{j=1}^n (\dot{m}_a w_c) \quad (7)$$

In which, n , \dot{m}_a and w_c are respectively the number of compressor stages, air mass flow rate through each compressor stage and its corresponding work. Considering adiabatic processes for the compressors, the exit temperature of each compressor stage ($T_{c,e}$) is calculated as [17]:

$$T_{c,e} = T_{c,i} \left[1 + \frac{r_c - 1}{\eta_{c,s}} \right] \quad (8)$$

Where, r_c stands for the compressor compression ratio, μ refers to the air specific heat ratio and $\eta_{c,s}$ is the compressor isentropic efficiency. $T_{c,i}$ is the inlet temperature of the relevant compressor

stage. The compressor specific work is then calculated using the first law of thermodynamics as the difference between inlet and exit enthalpies ($h_{c,i}$ and $h_{c,e}$):

$$w_c = h_{c,i} - h_{c,e} = c_{p,a}(T_{c,i} - T_{c,e}) \quad (9)$$

The second component of this configuration is the intercooling heat exchanger between the different stages of compressors. The heat extracted from the air stream through these heat exchangers is utilized for district heating purposes. For these heat exchangers, the inlet air temperature ($T_{a,i}$) is equal to the same stage compressor outlet air temperature. The outlet air temperature of the intercooler heat exchanger ($T_{a,e}$) is calculated by Ref. [18]:

$$T_{a,e} = T_{a,i}(1 - \varepsilon) + \varepsilon T_{w,i} \quad (10)$$

Here, $T_{w,i}$ is the heat exchanger inlet water temperature. Also, ε is the heat exchanger effectiveness. It is given by the following equations:

$$\varepsilon = \frac{NTU}{1 + NTU}; \text{ where: } NTU = \frac{UA}{C_{\min}} \quad (11)$$

Above, C_{\min} is the lower specific heat between the two fluids (air and water). U and A are also the overall heat transfer coefficient and heat transfer area, respectively. The heat rejected from the air stream, which is absorbed by the water stream and injected to district heating system, is calculated by:

$$\dot{Q}_{he} = \dot{m}_a c_{p,a}(T_{a,i} - T_{a,e}) \quad (12)$$

The mass flow rate of water that could be heated up by each heat exchanger is given by:

$$\dot{m}_w = \frac{\dot{Q}_{he}}{c_w(T_{w,e} - T_{w,i})} \quad (13)$$

In this equation, c_w is water specific heat (4179 J/kg.K). Note that the temperature of water entering the heat exchanger is 45 °C and its outlet temperature is set to 80 °C. The later represents a typical district heating supply temperature in Denmark [19], though next generation district heating may employ significantly lower supply temperatures, e.g. 55 °C [20].

Note that the same formulation, but with their own specific conditions, applies for the other heat exchangers in the system. However, for heating heat exchangers before the turbines, there are some other factors that should be calculated. For these heat exchangers, the mass flow rate of hot air outgoing from the thermal energy storage for each heating heat exchanger (\dot{m}_{ha}) is given by Ref. [18]:

$$\dot{m}_{ha} = \frac{\dot{m}_a(T_{a,e} - T_{a,i})}{(T_{ha,i} - T_{ha,e})} \quad (14)$$

In this equation, $T_{ha,i}$ is equal to the thermal energy storage temperature and $T_{ha,e}$ is the hot air outlet temperature from the heating heat exchangers calculable as [18]:

$$T_{ha,e} = T_{ha,i} - \frac{\varepsilon C_{\min}(T_{ha,i} - T_{a,i})}{\dot{m}_{ha} c_{p,ha}} \quad (15)$$

Where, ε is the heat exchanger effectiveness, C_{\min} is the lower value of heat capacity between the two fluid through the heat exchanger and $c_{p,ha}$ is the specific thermal capacity of heating air in constant pressure.

For the turbines, the inlet air temperature ($T_{t,i}$) is set on a constant as specific value. The heat required to increase the airflow

temperature up to this value is provided by the heat exchangers places before each stage of expansion. Considering an adiabatic process for each turbine, its outlet temperature is calculated as [17]:

$$T_{t,e} = T_{t,i} [1 + \eta_{t,s}(r_t - 1)] \quad (16)$$

Where, $\eta_{t,s}$ and r_t are the turbine isentropic efficiency and expansion ratio respectively. The turbine outlet temperature is then calculated as below:

$$w_t = h_{t,i} - h_{t,e} = c_{p,a}(T_{t,i} - T_{t,e}) \quad (17)$$

The total work done by the turbines set is also calculated by:

$$\dot{W}_t = \sum_{j=1}^n (\dot{m}_a w_t) \quad (18)$$

Thus, the net work of the system is:

$$\dot{W}_{\text{net}} = \dot{W}_t - \dot{W}_c = \dot{m}_a(w_t - w_c) \quad (19)$$

Clearly, the mass flow rate should be so high that the net work of the system could provide the power deficit (P_d) of the power plant. Thus:

$$\dot{m}_a = \frac{P_d}{\eta_g \dot{W}_{\text{net}}} \quad (20)$$

Where η_g is the electricity generator efficiency. Having the formulation above, one could define two sorts of efficiency for this system, namely, overall energy efficiency that consists of all energy types gained and spent in the system (heat and electricity) and electricity efficiency, which clearly just include the electricity output of the system versus the electricity input of the system. These are calculated respectively by the following correlations:

$$\eta_{\text{en}} = \frac{P_g + \sum \dot{Q}_w}{P_s} \quad (21)$$

$$\eta_{\text{el}} = \frac{P_g}{P_s} \quad (22)$$

In these two equations, P_g represents generated electricity by the energy storage system during an entire discharge process and P_s the total power consumption during a charging process. \dot{Q}_w is the heat transfer rate provided by each heat exchanger for district heating use.

2.2. Exergy analysis

Exergy (or availability, Ψ) is the maximum theoretical producible (minimum required) work from an entity, i.e. a stream or a specific amount of matter, as it passes from a given state to a dead state. The dead state is a state of the system that is in thermodynamic equilibrium with its environment. Normally, the dead state is taken as 298 K, 101.325 kPa and velocity and elevation relative to the environment equal to zero for many cases. The total exergy of an entity is equal to the summation of its physical, chemical, potential and kinetic exergies. Thus, indicating the dead state with the subscript o , Ψ is defined as [21]:

$$\Psi = m \left[(h - h_o) - T_o(s - s_o) + \psi^{\text{ch}} + \frac{V^2}{2} + gz \right] \quad (23)$$

Where, s , V and z are specific entropy, velocity and potential term, respectively and ψ is specific exergy. Note that m , in this

equation, is the total mass of the material that should be mass flow rate (\dot{m}) in case of having a fluid stream instead of a solid material. In this work, the kinetic and gravitational potential terms are considered negligible and chemical exergy is neglected as no chemical reaction is going to happen in the system.

The concept *irreversibility* for a system is defined as the rate of exergy destruction in the system due to entropy generation. It is calculated by subtracting the actual work of the system from its producible (required) work in a reversible process [21]:

$$\dot{I} = \dot{W}_{\text{rev}} - \dot{W}_{\text{act}} = T_0 \dot{S}_{\text{gen}} \quad (24)$$

The second law efficiency (η_{II}) is defined as [21]:

$$\begin{aligned} \eta_{II} &= \frac{\text{useful output availability}}{\text{input availability}} \\ &= 1 - \frac{\text{availability destruction and loss}}{\text{input availability}} \end{aligned} \quad (25)$$

Taking the fundamentals given for the exergy analysis, one could proceed to formulate all the system components one by one. Like in the energy analysis section, here also the cavern is the first component for exergy analysis modeling. The rate of exergy variation of the cavern over time can be calculated as [26]:

$$\dot{\Psi}_{\text{tes}} = \dot{m}[(h_i - h_e) - T_0(s_i - s_e)] - \left(1 - \frac{T_0}{T_{\text{tes}}}\right) \dot{Q}_1 \quad (26)$$

Irreversibility of the cavern, by doing an exergy balance, is given by Ref. [22]:

$$\dot{I} = T_0 \left[\dot{m}_a \left[c_{p,a} \ln \left(\frac{T_{a,i}}{T_{a,e}} \right) \right] - \dot{m}_{\text{tes}} \left[c_{p,\text{tes}} \ln \left(\frac{T_{\text{tes},2}}{T_{\text{tes},1}} \right) \right] - \frac{\dot{Q}_1}{T_{\text{tes}}} \right] \quad (27)$$

In this equation, $c_{p,\text{tes}}$ is the weighted average heat capacity of air and hot rocks within the cavern. For exergy efficiency of the cavern, three different cases, i.e. the charging exergy efficiency, the discharging exergy efficiency and the overall exergy efficiency, could be considered. For a total charging process, one has:

$$\eta_{II,\text{char}} = \frac{\text{total exergy stored in the cavern}}{\text{total exergy delivered in the cavern}} \quad (28)$$

For a complete discharging process, the exergy efficiency is defined as:

$$\eta_{II,\text{disch}} = \frac{\text{total exergy recovered from the cavern}}{\text{total exergy stored in the cavern}} \quad (29)$$

And finally, the overall exergy efficiency of the cavern is defined as the ratio of total exergy recovered from the cavern to the exergy delivered to that. Thus, one could write [22]:

$$\eta_{II,\text{tes}} = \eta_{II,\text{char}} \eta_{II,\text{disch}} = \frac{\Delta \Psi_{\text{disch}}}{\Delta \Psi_{\text{char}}}|_{\text{tes}} = \frac{(\Delta H - T_0 \Delta S)_{\text{disch}}}{(\Delta H - T_0 \Delta S)_{\text{char}}}|_{\text{tes}} \quad (30)$$

The second component of the system is the compressor set, which is going to be in operation in discharging step only. The rate of change in exergy for the air stream through the compressors can be simply given by Ref. [21]:

$$\dot{\Psi}_c = \dot{m}_a[(h_e - h_i) - T_0(s_e - s_i)] \quad (31)$$

In addition, the rate of irreversibility through the compressors is calculated by:

$$\dot{I}_c = T_0 \dot{m}_a \left[c_{p,a} \ln \left(\frac{T_{c,e}}{T_{c,i}} \right) - R_a \ln(r_c) \right] \quad (32)$$

Finally, defining the second law efficiency for a compressor as the ratio of exergy increase in the fluid through the compressor to the actual work of compressor, the compressor second law efficiency is calculated as:

$$\eta_{II,c} = 1 - \frac{T_0 \left[c_{p,a} \ln \left(\frac{T_{c,e}}{T_{c,i}} \right) - R_a \ln(r_c) \right]}{c_{p,a} (T_{c,e} - T_{c,i})} \quad (33)$$

For the water heat exchangers, which are only used during discharging, there are mainly two reasons for wasting availability. These are heat exchange across a finite difference temperature and fluid friction. The variation of exergy of both of the water and air streams are calculated by the same correlation as Eq. (31). Neglecting the pressure drop across the heat exchanger, the rate of irreversibility in these devices is given by Ref. [23]:

$$\dot{I}_{\text{hx}} = T_0 \left[\dot{m}_a c_{p,a} \ln \left(\frac{T_{a,e}}{T_{a,i}} \right) - \dot{m}_w c_w \ln \left(\frac{T_{w,e}}{T_{w,i}} \right) \right] \quad (34)$$

Defining the second law efficiency for a heat exchanger as the ratio of exergy increase in the cold fluid to exergy increase in the hot fluid, one has:

$$\eta_{II,\text{hx}} = \frac{\dot{m}_w c_w \left[(T_{w,e} - T_{w,i}) - T_0 \ln \left(\frac{T_{w,e}}{T_{w,i}} \right) \right]}{\dot{m}_a c_{p,a} \left[(T_{a,i} - T_{a,e}) - T_0 \ln \left(\frac{T_{a,i}}{T_{a,e}} \right) \right]} \quad (35)$$

Note that the same formulation applies for the heating heat exchangers.

For the turbine set Eq. (31) can also be employed for calculating the variation of exergy through the device. Having the variation of exergy, one can calculate the turbine irreversibility by Ref. [17]:

$$\dot{I}_t = T_0 \dot{m}_a \left[c_{p,a} \ln \left(\frac{T_{t,i}}{T_{t,e}} \right) - R_a \ln(r_t) \right] \quad (36)$$

The second law efficiency of each turbine is defined as the ratio of the actual work of the turbine to the amount of decrease in the availability of air through the turbine. Thus:

$$\eta_{II,t} = \frac{c_{p,a} (T_{t,i} - T_{t,e})}{c_{p,a} (T_{t,i} - T_{t,e}) - T_0 \left[c_{p,a} \ln \left(\frac{T_{t,i}}{T_{t,e}} \right) - R_a \ln(r_t) \right]} \quad (37)$$

Finally, having the exergetic performance details of each component in the system, the second law efficiency of the whole system for a complete charging and discharging process is defined as:

$$\eta_{II,\text{ESS}} = \frac{P_g + \sum \dot{Q}_w \left(1 - \frac{T_0}{T_w} \right)}{\dot{Q}_s \left(1 - \frac{T_0}{T_{\text{tes}}} \right)} \quad (38)$$

In which, \dot{Q}_s and T_{tes} are respectively the surplus energy supplied for the system in form of heat ($\dot{Q}_s = P_s$) and the cavern temperature at which this heat is injected to the cavern. T_w is also the temperature at which heat is provided for water for district heating purposes. Note that temperatures in Kelvin must be applied to these equations.

Table 1 presents information about the physical and technical properties of different components of the energy storage system considered in this work.

Table 1
Physical and technical properties of different components of system [9].

Parameters Value	Symbol (Unit)	Remarks
Height of the cavern	H (m)	10 m
Radius of the cavern	R (m)	30 m
Density of the rock	ρ_r (kg/m ³)	2700.0
Thermal conductivity of the rock	k_r (W/m.K)	3.0
Specific heat of the rock	c_r (J/kg.K)	862.0
Porosity of packed bed	ϵ	0.35
Volumetric heat transfer coefficient	h_v (W/m ³ .K)	1029.7
Thermal conductivity of the insulator	k_{ins} (W/m.K)	0.04
Thickness of the insulator	δ_{ins} (m)	1
Inlet temperature in the charging mode	$T_{c,in}$ (°C)	675
Maximum allowable temperature of cavern	$T_{tes,max}$ (K)	950
Cavern volume	V_{tes} (m ³)	225000
Heat exchangers effectiveness	ϵ	0.8
Number of compression/expansion stages	–	3
Compressors/turbines isentropic efficiency	η_{is}	85%
Electricity generator efficiency	η_G	95%
Target temperature of turbines inlet air	T_{ti} (K)	823
Nominal charging power (maximum surplus power)	$P_{s,n}$ (MW)	100
Nominal discharging power (maximum recoverable deficit power)	$P_{d,n}$ (MW)	100
Inlet temperature of water heat exchangers	$T_{w,i}$ (°C)	45
Target temperature of water heat exchangers	$T_{w,e}$ (°C)	80

3. Results and discussions

In this section, the results of dynamic simulations and the details of an optimized HTHPSS system are presented and comprehensively discussed. This study includes economic aspects of employing a storage unit in combination with wind turbines in the electricity and heat markets local to Aarhus, Denmark. Thus, dynamic electricity prices at various time scales [14], hourly heat prices for Aarhus city [24] and historical 5-min electricity system data [14] of the West Denmark market over 2015 are taken into account. In addition, the hourly ambient temperature, which affects the level of heat losses from the cavern and also the compressor set efficiency are taken from a measurement station operated by the Aarhus district heating company [24]. Fig. 3 presents information about the hourly electricity and heat prices and ambient temperature described above.

The ambient temperature varies between a maximum of 30 °C in summer and a minimum –5 °C winter. The extremes are rarely observed. These variations do not impact the system performance significantly, but are included in the simulation nevertheless. The electricity production price varies between about –200 and 600 DKK (26.9–80.6 €) per MWh, but most frequently it falls

between about 50 and 200 DKK (6.7–26.9 €) per MWh. It fluctuates at multiple time scales including daily fluctuations and a seasonal trend. The later shows higher average prices during the colder months of the year compared to the average price of electricity in summer. The heat price varies around 250 DKK (33.6 €) per MWh and shows similar, but not identical daily and seasonal trends. It occasionally exhibits a sharp increase in the heat price, e.g. late spring and early fall. These jumps are caused by times when the main heat production plant stops normal operation for any reason, e.g. maintenance or pipe or pump failure. In such cases, back-up oil boilers are employed for providing the district heating network demand.

3.1. Combined storage and wind turbine bidding strategy

One of the main goals of this article is to present a dynamic modeling of the performance of the combined wind and HTHPSS illustrated in Fig. 1. However, detailed optimization of the charging and discharging strategy of the energy storage system is out of scope of this work. A compromise that is more accurate than simple averaging methods based on prognosis data is an efficient, but not fully optimal algorithm for the system operation strategy. In the

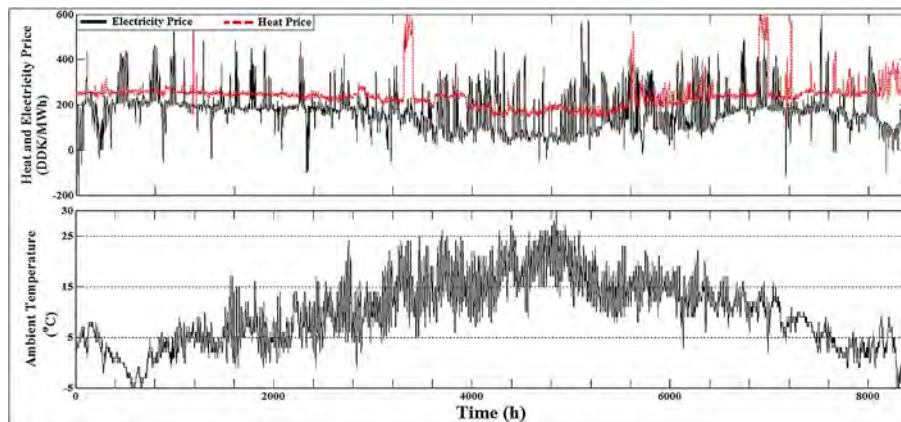


Fig. 3. The upper panel shows hourly electricity (black) and heat (red) production prices for 2015. The lower panel shows ambient temperature of West-DK in 2015. (For interpretation of the references to colour in this figure legend, the reader is referred to the web version of this article.)

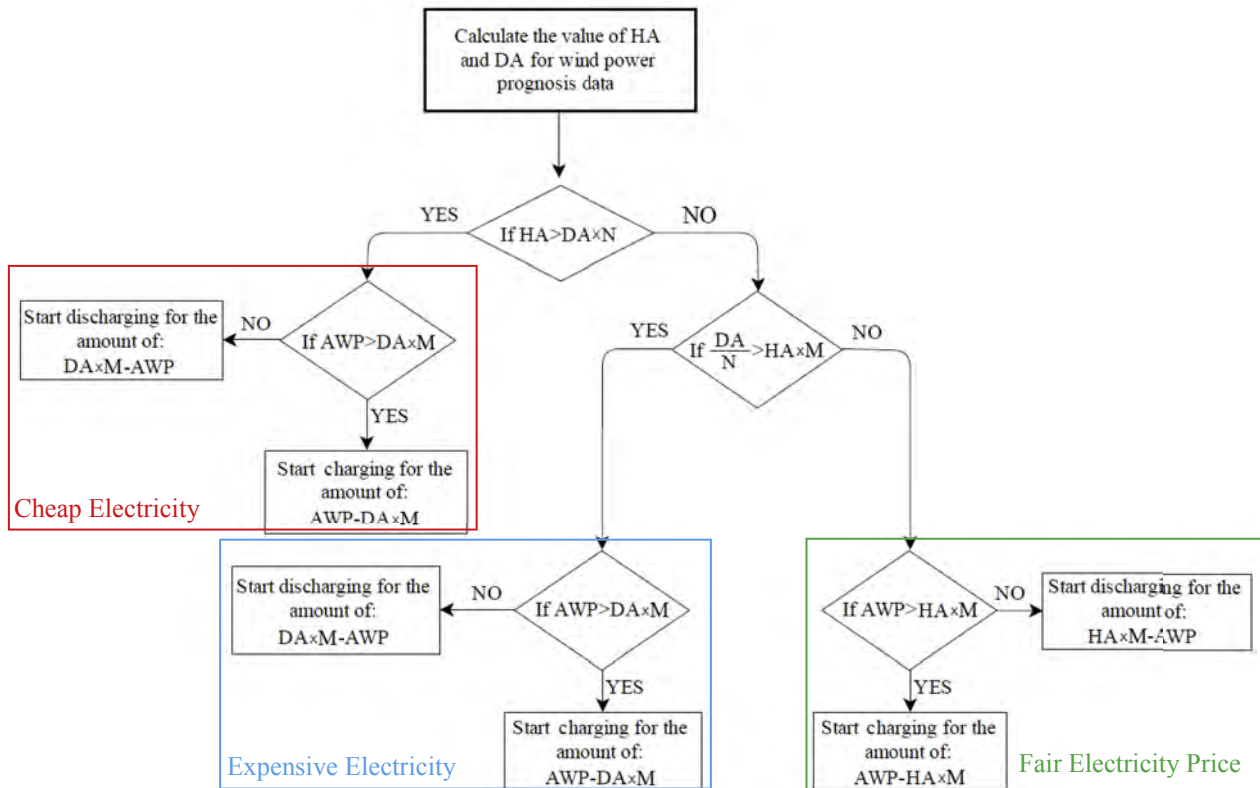


Fig. 4. The algorithm for bidding in the day-ahead market for the combined wind turbine and energy storage system; DA: Forecast of the daily average wind power generation, HA: Forecast of the hourly average wind power generation, N and M: constant coefficients, AWP: actual wind power generation at 5 min resolution.

following, the applied algorithm is described. It is illustrated in Fig. 4.

Most importantly, the storage system acts to compensate wind power forecast uncertainties and to stabilize the fluctuating power output from wind turbines. Secondly, it operates to shift electricity from high wind periods to low wind periods. This is achieved in the following way: First forecasted wind power generation with hourly resolution (HA) is used to develop forecasted daily average power production data (DA). Then, two constants N and M are used to together with DA and HA to specify the periods of charging and discharging for the energy storage system. In this way, low and high electricity price periods of each day can be estimated with a good accuracy because, during periods with high availability of wind power ($HA \gg DA$) the electricity price is very low and vice versa if $DA \gg HA$, then electricity is likely to be expensive. For both of these cases, $M \times DA$, where $0\% < M \leq 100\%$, are considered the bidding value in day-ahead market. There may be also a third case, i.e. fair electricity price periods when HA is neither much higher nor much lower than DA. For this case, wind turbines bid the value $M \times HA$.

By simulating the system over a whole year based on this algorithm, one could propose the optimal values of N and M based on the maximum annual net income of the system. Note that the power sales levels in day-ahead market should be based on constant hourly values.

Fig. 5 shows the net annual benefit of operation of the energy storage system and bidding strategy for various values of M and N. According to the figure, the net annual benefit is higher for lower values of N and it is in its peak when N is practically equal to 1. On the other hand, different profiles associated with various N values, the maximum benefit is obtained for M values of about 0.85 and

decrease significantly for lower and higher values. Thus, for this case study the following values are used $N_{opt} = 1$ and $M_{opt} = 0.85$.

Also, for the sake of proving the effect of selecting an appropriate M value for this algorithm, Fig. 6 shows the variation of energy, electricity and exergy efficiencies as well as the proportion of non-recoverable power deficits (coverage capability) in the system for changing values of M. All of these parameters are very important in the operation of the energy storage system, especially the coverage capability that strongly affects the justifiability of employing an energy storage system. As can be seen, there is sharp increase in all the efficiencies when the value of M changes from 0.75 to 0.85 while the values of efficiencies (all the three sorts of efficiencies) get almost flat thereafter. In contrast, the non-recoverable ramps for values of M greater than 0.85 increases rapidly. The economic performance of the storage favors high efficiencies and a low number of non-recoverable ramps. This means that optimal values of N and M are well explained by the underlying technical performance of the system, which implies that the particular details of the economic modeling are not biasing the results to a large extent.

Fig. 7 presents information about the hourly and daily average of wind power production prognosis data in the region in West Denmark in 2015. As seen, there is good agreement between the predicted values and realized amount of wind production in most of the time, except a few periods, at the end of the year particularly in which the deviation looks too much.

Taking advantage of the developed algorithm and the data presented in previous figure, one could define the optimal bidding value for the wind farm in day-ahead market and operating (charging and discharging) strategy for the energy storage system during the year. Fig. 8(A) presents information about the practically

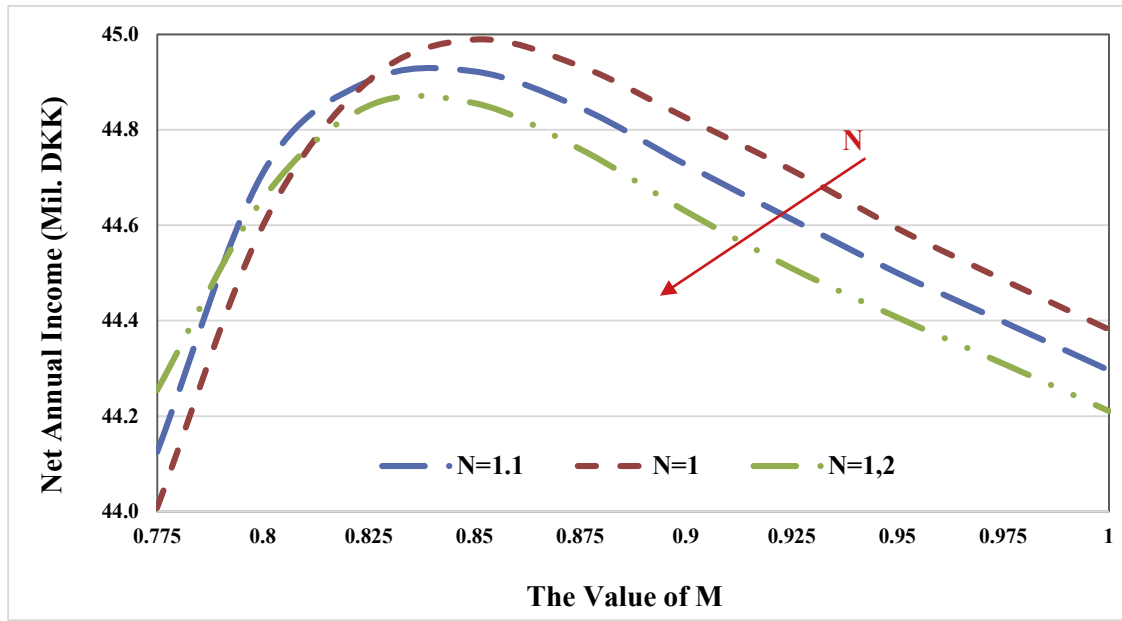


Fig. 5. The optimal values of M and N for the algorithm of bidding in day ahead market and operation of energy storage system.

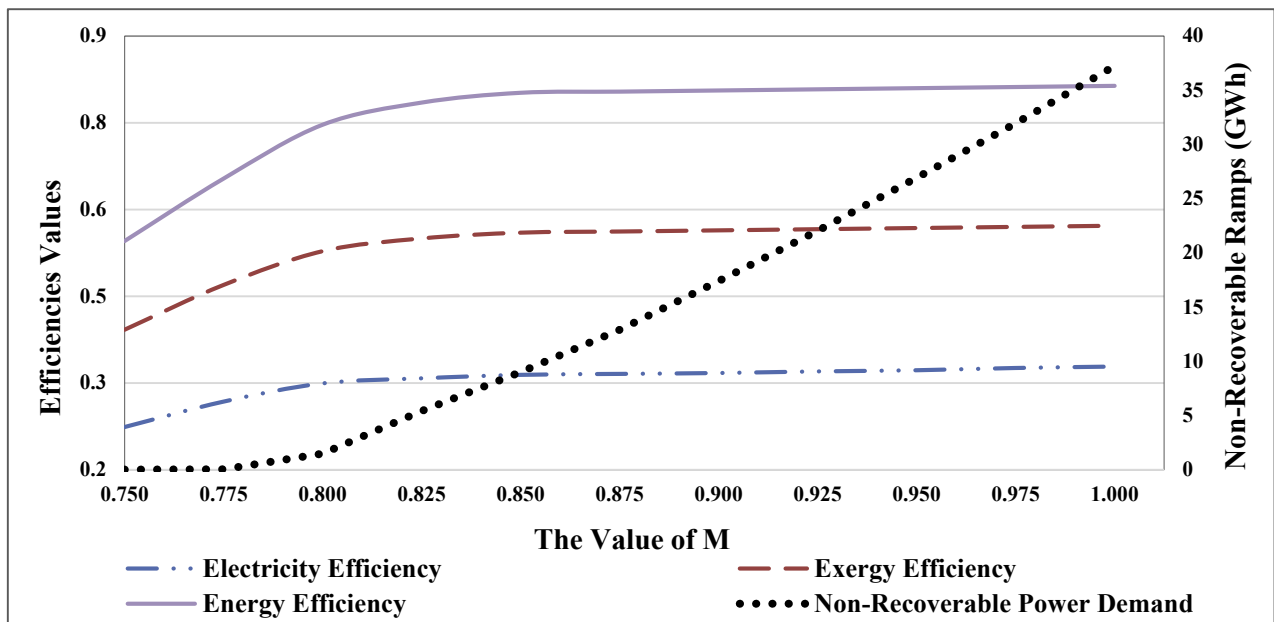


Fig. 6. The effect of selecting the optimal value of M on the energy (N = 1), exergy and electricity efficiency of the energy storage system as well as its power deficit coverage capability.

produced wind power in the case study in 5-min time steps (the red graph) and the value based on which the power plant bids in the day-ahead market (the black line). Also, Fig. 8(B) magnifies a sample of three selected days of the year (days 101–103) to show the operational strategy of the energy storage system. In this figure, the green area shows the charging level and period while the red area shows the amount and period of discharging.

Clearly, even in case of optimizing the operation strategy of the system, due to the limited capacity of the storage, there can be still some periods in the system that energy deficits of the power plant cannot be efficiently recovered by the energy storage system. These points are in fact those periods during which the hot rock cavern

temperature falls below 600 °C and system, and even in case of an electricity deficit, it stops producing electricity and it shifts to charging mode if there is surplus power available. Fig. 9 shows the levels of unrecovered ramps in the system. As can be seen, there are very few points over the year that the energy storage system cannot support the wind turbine farm to stick on the bided power value in the day-ahead market. In fact, this figure confirms the reliability of the system shown by Fig. 6 that shows successful power deficit coverage proportion of almost 94%. According to the figure, below 2% of the time in the year the power deficit in the system could not be covered.

Fig. 10 illustrates the variation of hot rock cavern temperature

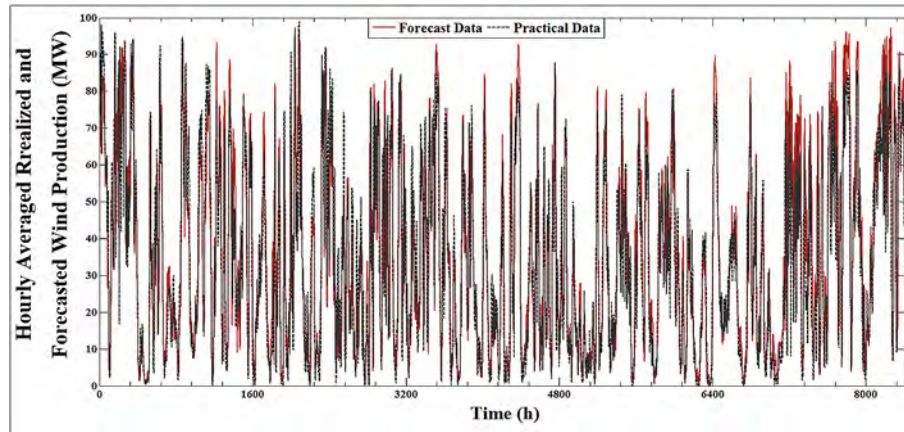


Fig. 7. The hourly averaged realized and forecasted wind production in West Denmark (scaled in 100 MWp).

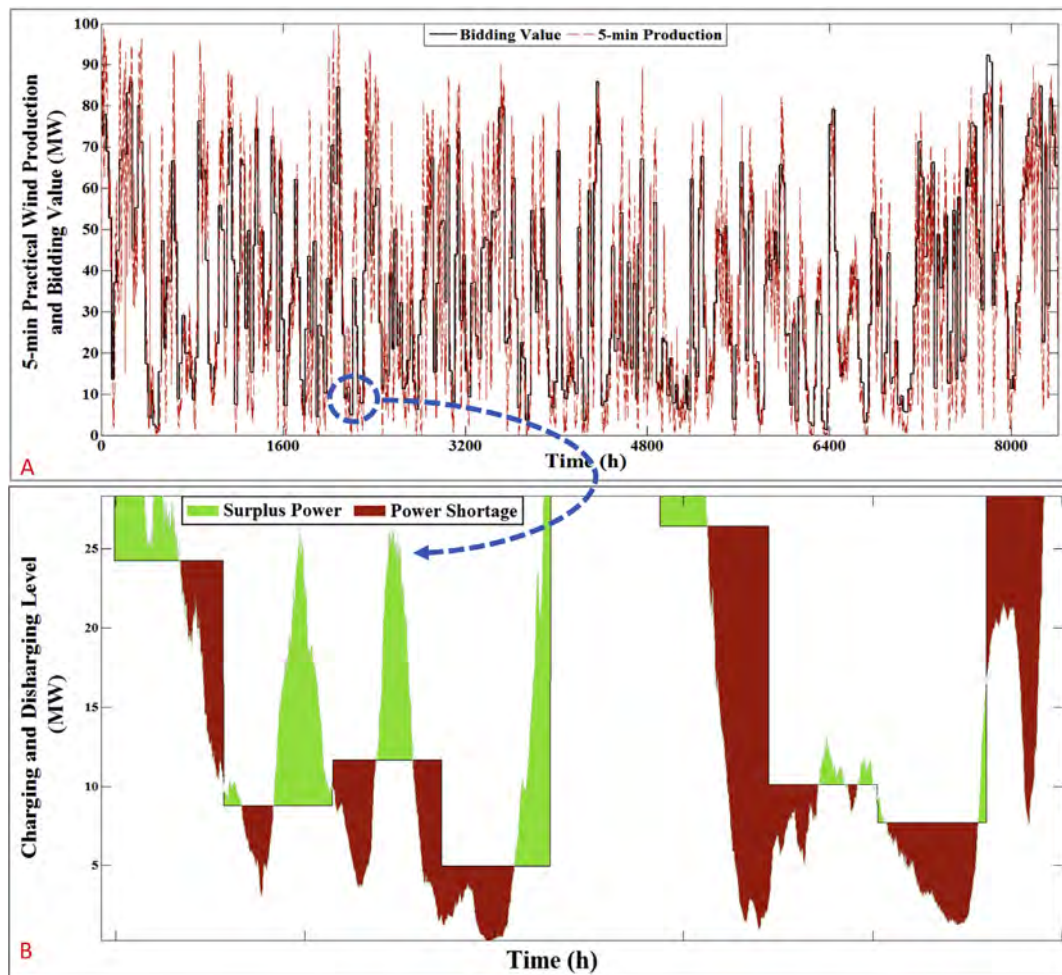


Fig. 8. 5-min wind power production data and the bidding value in day ahead market (A) and the magnified version of three sample days to show the practical charging and discharging strategy (B).

based on 5-min data over the whole year. As can be seen, the maximum temperature of the storage throughout the year is 675 °C (950 K). Also, it can be seen that the cavern temperature is still higher than its initial temperature of 600 °C at the end of the year (607 °C) and it means that the cavern has not been over discharged during the year and also there is still a little not used stored energy

available in the cavern for the next year. Due to the fluctuations of temperature in the storage system, maximum and average heat loss rates of 1367 kW and 1274 kW occur over the year. It is bears mentioning that as heat loss from the cavern to the environment is a direct function of the cavern temperature, its trend is almost the same as cavern temperature trend and this is why this graph is not

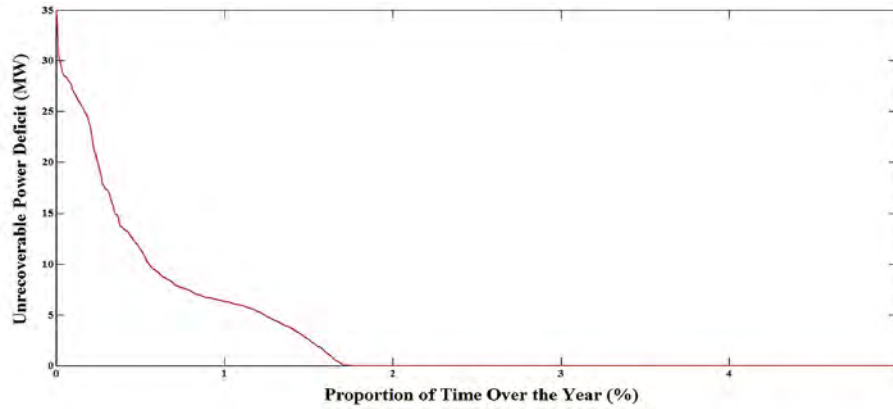


Fig. 9. Wind power deficit not compensated by the energy storage system.

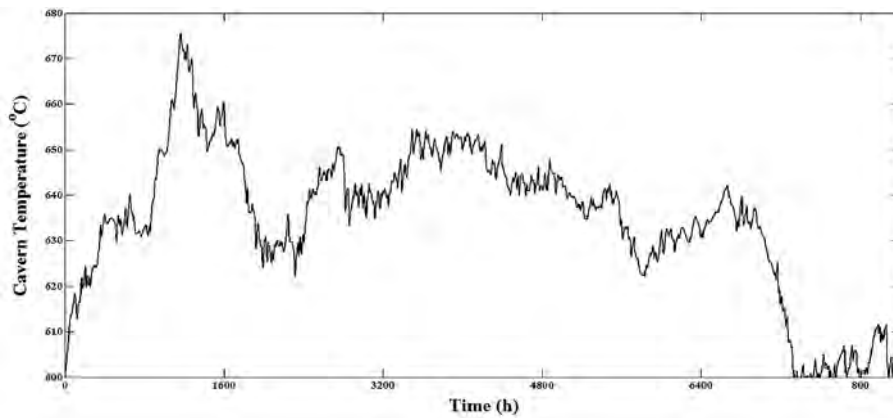


Fig. 10. Hot rock cavern temperature over an entire year of operation.

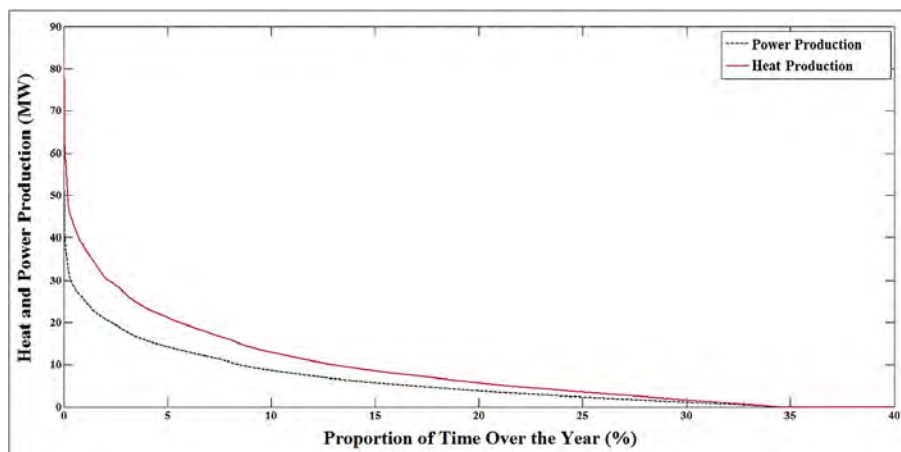


Fig. 11. The rate of heat and electricity production by the energy storage system over the year.

presented here.

Fig. 11 shows the amount of produced heat and electricity over the year. As can be seen, the rate of heat production is always higher than electricity production and this is why overall energy efficiency is higher than double times of electricity efficiency.

Table 2 gives detailed information and statistics about the results of analysis accomplished on the performance on the energy storage system during the year.

3.2. Energy and exergy performance

In the following, a dynamic exergy and irreversibility analysis of each component of system is presented. In this regard, Fig. 12(a–d) presents duration curves of the rate of irreversibility in the cavern, the rate of exergy and irreversibility of the turbines and compressors. These curves show the value of the given components versus the proportion of time during the year.

Table 2
The system performance analysis results.

Parameter	Value (GWh)
Total storage charging energy	61.1
Total electricity deficit recovered	26.9
Total unrecovered electricity ramps	9.0
Total heat produced for district heating	29.5
Total heat lost from the hot rock cavern	6.6
Total worked produced by turbines	43.7
Total worked consumed by compressors	24.8

According to figure, the increase in exergy of airflow is higher through the later stages of the compressor set because the inlet temperature of each stage is higher than the previous stage and as a result, the outlet temperature is also higher. Also, it is shown that, the compressors only work up to 35% of the year. As irreversibility is a functional of the compressors outlet to inlet temperatures and as the ratio of outlet temperature to the inlet temperature of all the compressors are the same, its value for all of the compressors are equal as temperature ratio is equal for the compressor stages. Thus, this figure presents the irreversibility of one stage of the compressors only. The maximum of irreversibility is almost 2.5 MW, which rarely occurs and irreversibility rates higher than 1 MW are observed during only 3% of the time during the year (Fig. 12-a).

Fig. 12-b is associated with airflow exergy reduction and irreversibility through the turbines. These two parameters are presented for one of the turbines only because operational condition of all the turbines are assumed to be exactly the same. Thus, their rate of irreversibility as well as the rate of exergy change through them are exactly the same. Note that, the rate of exergy variation of airflow through the turbines is decreasing; therefore, the values given by the black curve should be considered as negative values. According to the figure, a maximum of 20 MW exergy reduction through each turbine is expected, though exergy reduction levels above 6 MW in airflow rarely occurs (only 5% of the time). On the other hand, for the rate of irreversibility, a maximum of around 2 MW could be observed and for 95% of the time, the irreversibility rate is below 700 kW. Finally, Fig. 12-d shows the rate of irreversibility of the hot rock cavern. As seen, it is very small in comparison with the other parts of the system.

Similarly, Fig. 13(a and b) shows the rate of irreversibility in the heating heat exchangers and water (district heating) heat exchangers. For the heating heat exchangers (Fig. 13-a), due to the similarity of the operating conditions of the second and third heating heat exchangers, the results associated with one of them is only presented. As can be seen, the rate of irreversibility through

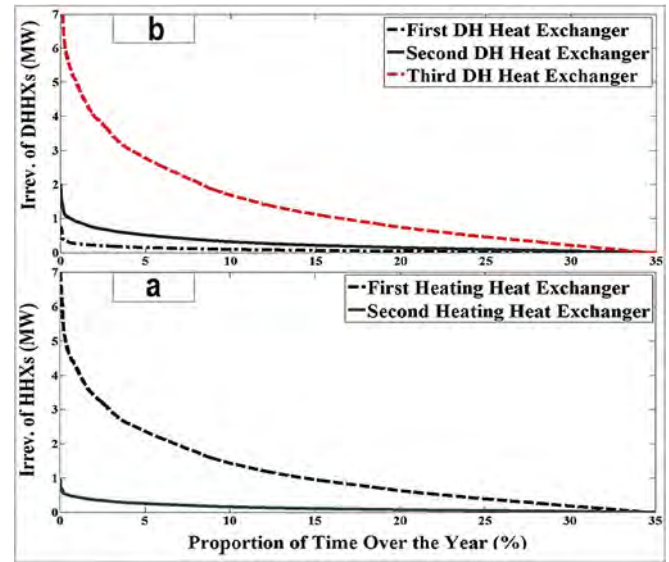


Fig. 13. The rate of irreversibility in district heating heat exchangers (a) and heating heat exchangers (b).

the first heating heat exchanger is much higher (up to 7 MW) than the later stage heating heat exchangers, which have irreversibility levels below 1 MW. The reason is that the temperature difference of airflows on the two sides of the first heat exchanger is much higher than of later stages, which work in lower temperature gradient ranges. For the water heat exchangers (Fig. 13-b), the level of irreversibility in the last stage water heat exchanger is much higher as temperature gradient of the inlet and outlet of the heat exchanger is much higher than the other two cases. The maximum irreversibility rate in the last district heating heat exchanger is well above 7 MW while its value for the first and second district heating heat exchangers is respectively 1.8 MW and 0.7 MW.

Given the above results, the components with the most significant irreversibility rates can be identified. This information can be used to prioritize which of the devices that would benefit the most from optimization. Overall, the first heating heat exchanger and the last district heating heat exchanger could result in considerable enhancement in exergy efficiency of the whole system rather than the other heat exchangers. For the compressors and turbines also, all the three stages are in the same degree of importance for being optimized, though they seem efficient enough and not much enhancement could be done on them. The last priority is with the

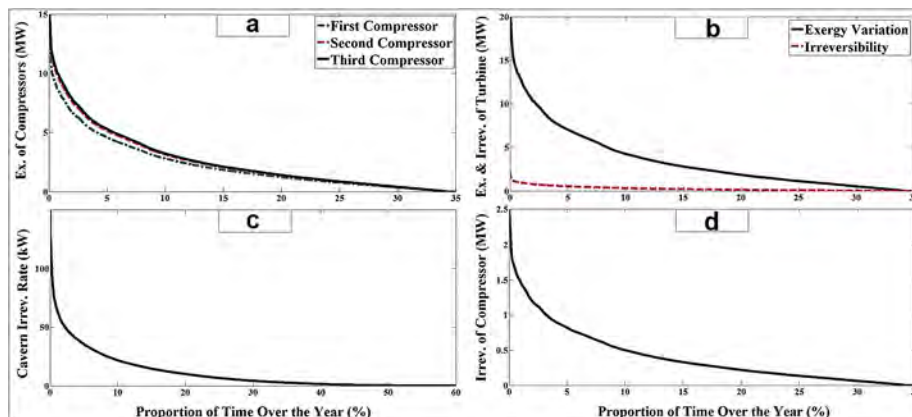


Fig. 12. Exergy and Irreversibility of various components in the system.

cavern, which is highly efficient in terms of exergy performance.

Having the presented information about energy and exergy performance of different devices in the system, one can calculate the value of energy (heat and electricity) and exergy efficiencies (electricity) of the whole system for an entire year of operation. Fig. 14 present this information for the proposed system and compares this system with batteries and compressed air energy storage system as two of best energy storage systems proposed so far.

According to the figure, an exergy efficiency of 56.1%, electricity production efficiency of 31.4% and high overall energy (both heat and electricity) efficiency of 80.2% is expected from the system. As expected, battery presents better performance in all terms. However, as mentioned before, the problem of batteries are that they are technically and economically difficult to scale to the large capacities required to support integration of surplus renewable energy. For grid support at short time scales batteries are an effective option. Comparing HTHPSS to compressed air technology, electricity production efficiency of compressed air is much higher, but the overall energy efficiency of HTHPSS is almost 10% better. The exergy efficiencies are similar. In addition, much lower capital cost, not being geographically restricted (for reservoir excavation) and simpler technology (much lower operational pressure) are the other advantages of HTHPSS relative to compressed air energy storage system. Thus, considering close heat and electricity prices, which is somewhat reasonable in Denmark, and taking the above-mentioned advantages, the proposed system outperforms compressed air technology as well. Note that the values of efficiencies for battery and compressed air energy storage system were adopted from Refs. [25] [26], respectively.

3.3. Economic performance

In this section, market value estimates of a 100 MWp stand-alone wind turbine system are compared with those of a similar system equipped with a storage system as detailed in Table 1 and operated as described in Fig. 4. In both cases, the wind turbines create value by direct power sales, but for the storage system, additional value is created by letting it: i) shifting production from high to low wind periods, ii) compensate the difference between the forecasted hourly wind power production and the realized hourly production, iii) balance the intra-hour variations of the wind power generation, and iv) produce heat for district heating

purposes as a bi-product of these actions.

The system value of the produced electricity from each of the two systems is divided into three categories to distinguish the effect of day-ahead power sales; intra-day trades to compensate forecast errors and real-time balancing at short time scales. In the day-ahead market, each system bids in their forecasted hourly production (P_{bid}) for which they receive the so-called hourly spot price (V_{spot}) that the market settles on (see Fig. 3). The annual value in the day-ahead market is calculated as:

$$\text{Value in day - ahead market} = \sum_t P_{bid}(t) V_{spot}(t) \quad (39)$$

After the day-ahead market close and up to 1 h before actual production, producers and consumers trade their expected imbalances in the intra-day market. For wind power, in particular, updated forecasts may guide this trade. Here, we assume that the difference between the hourly average values of the day-ahead estimated production (P_{bid}) and the realized hourly average production (P_{real}) is traded in this market. In cases where $P_{bid} > P_{real}$, the system has to procure additional energy in the intra-day market, while the additional energy can be sold in the opposite case where $P_{bid} \leq P_{real}$. In either case, the trade is assumed to occur at the hourly spot price (V_{spot}). This choice is statistically consistent with hourly 2015 prices in the Elbas (intra-day) market for Denmark West [14], although it ignores the relatively large fluctuations around the average price. With these choices, the annual value in the intra-day market is calculated as:

$$\text{Value in intra - day market} = - \sum_t (P_{bid}(t) - P_{real}(t)) V_{spot}(t) \quad (40)$$

Real-time balancing at time-scales shorter than 1 h is handled by the system operators through the procurement of a number of different reserves. Here, we treat all different types of reserves in a simplified way where we only consider the 5-min variations (P_{5-min}) around the average hourly production (P_{real}). Based on price data from Ref. [14], we find that up balancing should be priced at 100 DKK (13.4 €) above the spot price and down balancing at 100 DKK (13.4 €) less than the spot price. Over a whole year, the value in the real-time market is estimated as:

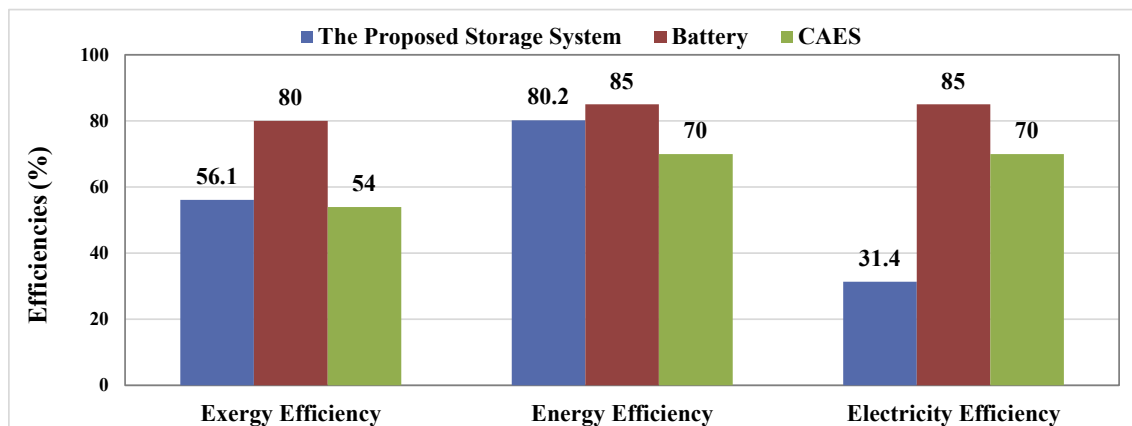


Fig. 14. The annual energy and exergy efficiencies of the whole system and comparison with other storage systems.

Table 3

The economic outcomes of employing the energy storage system relative to direct wind power sales method.

Parameter	Stand-Alone Wind Turbines (1000 €)	Wind Turbine with HTHPSS (1000 €)	Difference (1000 €)
Value in day-ahead market	6094	5302	–792
Value in intra-day market	–201	–148	54
Value in intra-hour market	–161	–13	148
Value in heat market	0	966	966
Total value	5732	6107	362

$$\begin{aligned} \text{Value in real-time market} = & - \sum_t \frac{1h}{12} \sum_{i=1}^{12} (\\ & \times |\Delta_{5-\min}(t, i)| V_{\text{spot}}(t) \\ & + \Delta_{5-\min}(t, i) \times 100 \text{ DKK}) \end{aligned} \quad (41)$$

where, $\Delta_{5-\min}(t, i) = P_{\text{real}}(t) - P_{5-\min}(t, i)$ denotes the power during the i 'th 5-min interval in a given hour t . Note that unlike the intra-day market in which additional power can create positive value, both up and down regulation has a negative value in the real-time market.

In the heat market, the storage system is considered a price taker without balancing responsibility. This means that it will receive the average production price (V_{heat}) for each hour (see Fig. 3). The annual value of produced heat is thus calculated by:

$$\text{Value in heat market} = \sum_t P_{\text{heat}}(t) V_{\text{heat}}(t) \quad (42)$$

The total annual value in each of the markets is summarized in Table 3 for the stand-alone wind turbine system and for the combined wind and HTHPSS system. The stand-alone wind turbine system has a 15% higher value in the day-ahead market compared to the combined system. This is because the direct power sales are higher as the electricity-to-electricity round trip efficiency of the HTHPSS is about 31%. The combined system, on the other hand, performs better in the intra-day and intra-hour markets as the storage system acts to compensate wind forecast errors as well as intra-hour variations. Combining all electricity markets the advantage of the stand-alone wind system is about 14%. The combined system, however, has a significant value in the heat market where the wind turbines are not present. This more than compensates the loss in the electricity markets, and the total value in all markets combined is about 6% higher for the combined system in the present case study. It is conceivable that this number can be increased if the storage dispatch strategy is further optimized. In addition, the storage system would benefit relatively more from future increases in price volatility, which typically occurs with increasing shares of renewable energy. More importantly, the combined system address the problem of financing active upwards capacity in an energy system with high shares of weather driven renewable energy. As described in the introduction, wind and solar sources are not able to replace capacity reserves to a large extent, but in systems where they are present, the business case of traditional power plants is challenged as their production pattern goes from regular base-load and peak-load production to irregular peak-load production. The combined HTHPSS and wind turbine system, on the other hand, is able to generate a positive value during most of the year by compensating wind forecast errors and stabilizing its fluctuating power generation as well as by producing valuable heat. With proper scheduling these systems will also be able to provide power during the irregular periods of low wind and solar power generation.

4. Conclusions

The novel and simple yet efficient system of HTHPSS (High Temperature Heat and Power Storage System) suitable for the locations with high heating demand as well as electricity demand was previously proposed and investigated in terms of economic justification by the authors [9]. In the present work, a detailed dynamic energy and exergy modeling of this energy storage unit in combination with wind turbines is presented to evaluate to what extent it is efficient enough for long term storage with dynamic power supply and energy output. For this objective, an efficient operational (charging and discharging) strategy algorithm was developed for an energy storage system with 100 MW capacity supporting a wind turbine farm with maximum power production capacity of 100 MWp in Denmark-West as the case study of this work. The investigations showed that both energy and exergy efficiencies are in very good levels. In addition, the most important sources of energy loss and exergy destructions are identified to guide optimization and practical efforts to enhance the levels of obtainable efficiencies. For example, in the heat exchangers, higher temperature difference between the inlet and outlet conditions make considerable amount of irreversibility in the system, thus optimizing the heat exchange methodology may increase the efficiency of the system significantly. Also, energy losses from the cavern are extremely high due to the very high temperature of storage and minimizing heat losses by employing better insulation materials may help to achieve better efficiency. Another important point is that the algorithm developed for defining the operational strategy of the system is not the optimal case and it is expected that a more accurate algorithm, for specifying the system charging (low electricity price) and discharge (high electricity and electricity price) periods, makes the system more efficient technically and economically. This would be a multi-optimization algorithm as all of the effective parameters of the system operation, i.e. wind power, electricity price and heat price, fluctuate sharply.

The economic performance of the combined HTHPSS and wind turbine system was assessed by estimating the system value in the electricity and heat markets. This showed higher direct electricity sales for a stand-alone wind turbine system, but since the combined system is able to avoid losses in the intra-day and intra-hour electricity markets and produce heat along with electricity, it made a total annual income of almost 7% higher.

References

- [1] Vores Energy: <http://www.projectzero.dk/Files/files/dokumenter/vores%20energi%20-%20web.pdf>, last (Accessed 29 November 2016).
- [2] Mathiesen BV, Lund H, Connolly D, Wenzel H, Østergaard PA, Möller B, et al. Smart energy systems for coherent 100% renewable energy and transport solutions. *Appl Energy* 1 May 2015;145:139–54.
- [3] Arabkoohsar A, Machado L, Farzaneh-Gord M, Koury RNN. Thermo-economic analysis and sizing of a PV plant equipped with a compressed air energy storage system. *Renew Energy* 2015;83:491–509.
- [4] Suberu MY, Mustafa MW, Bashir N. Energy storage systems for renewable energy power sector integration and mitigation of intermittency. *Renew Sustain Energy Rev* 2014;35:499–514.
- [5] Kyriakopoulos GL, Arabatzis G. Electrical energy storage systems in electricity generation: energy policies, innovative technologies, and regulatory regimes.

- Renew Sustain Energy Rev 2016;56:1044–67.
- [6] Chen H, Cong TN, Yang W, Tan C, Li Y, Ding Y. Progress in electrical energy storage system: a critical review. *Prog Nat Sci* 2009;19:291–312.
- [7] Yang CJ. Chapter 2-pumped hydroelectric storage. *Storing Energy* 2016: 25–38.
- [8] Arabkoohsar A, Machado L, Koury RNN. Operation analysis of a photovoltaic plant integrated with a compressed air energy storage system and a city gate station. *Energy* 1 March 2016;98:78–91.
- [9] Arabkoohsar A, Andresen GB. A simple yet efficient energy storage system operating based on a thermal energy storage approach. *Energy* 2017;126: 21–33.
- [10] Andresen GB, Rodriguez RA, Becker S, Greiner M. The potential for arbitrage of wind and solar surplus power in Denmark. *Energy* 2014;76:49–58.
- [11] Ziel F, Steinert R, Husmann S. Forecasting day ahead electricity spot prices: the impact of the EXAA to other European electricity markets. *Energy Econ* 2015;51:430–44.
- [12] Qureshi N. An analysis of bidding strategies in the Danish wind power market. Master thesis. Norwegian University of Life Sciences; 2014. Permanent link, <http://hdl.handle.net/11250/217351>.
- [13] Zhao P, Wang J, Dai Y. Capacity allocation of a hybrid energy storage system for power system peak shaving at high wind power penetration level. *Renew Energy* 2015;75:541–9.
- [14] Energinet: <http://energinet.dk/EN/El/Engrosmarked/Udtraek-af-markedsdata/Sider/default.aspx>, Last (Accessed 29 November 2016).
- [15] Park JW, Park D, Ryu DW, Choi BH, Park ES. Analysis on heat transfer and heat loss characteristics of rock cavern thermal energy storage. *Eng Geol* 2014;181: 142–56.
- [16] Fchart website providing the EES software: <http://www.fchart.com/ees/>.
- [17] Arabkoohsar A, Machado L, Farzaneh-Gord M, Koury RNN. The first and second law analysis of a grid connected photovoltaic plant equipped with a compressed air energy storage unit. *Energy* 2015;87:520–39.
- [18] Bergam TL, Lavine AS, Incropera FP, DeWitt DP. Fundamentals of heat and mass transfer. seventh ed. New York: John Wiley & Sons; 2011.
- [19] http://www.ens.dk/sites/ens.dk/files/climate-co2/Global-Cooperation/Publications/dh_danish_experiences180615.pdf, last (Accessed 29 November 2016).
- [20] Lund Henrik, Werner Sven, Wiltshire Robin, Svendsen Svend, Thorsen Jan Eric, Hvelplund Frede, et al. 4th generation district heating (4GDH): integrating smart thermal grids into future sustainable energy systems. *Energy* 15 April 2014;68:1–11.
- [21] Bejan A. Fundamentals of exergy analysis, entropy generation minimization, and the generation of flow architecture. *Int J Energy Res* 2002;26:545–65.
- [22] Li G. Sensible heat thermal storage energy and exergy performance evaluations. *Renew Sustain Energy Rev* 2016;53:897–923.
- [23] Shah RK, Seculic DP. Fundamentals of heat exchanger design. John Wiley & Sons; 2003. ISBN: 0-471-32171-0.
- [24] Aarhus district heating Company: <http://www.aarhus.dk/sitecore/content/Subsites/affaldvarmeaarhus/Home.aspx>.
- [25] Rosen Marc A, Bulucea Cornelia Aida. Using exergy to understand and improve the efficiency of electrical power technologies. *Entropy* 2009;11: 820–35. <http://dx.doi.org/10.3390/e11040820>.
- [26] Hossein Safaei T, Aziz Michael J. Thermodynamic analysis of a compressed energy storage facility exporting compression heat to an external heat load. In: Proceedings of ASME 2014, 12th biennial conference on engineering systems design and analysis. Copenhagen, Denmark: ESDA; June25–27, 2014.

Nomenclature

A: Area/Cross sectional area of cavern (m²)

c: Specific heat capacity (W/m²)
 c_p : Specific thermal capacity in constant pressure (kJ/kg °C)
 D: Cavern diameter (m)
 d: Equivalent diameter of cavern (m)
 DKK: Danish Krone currency
 E: Internal Energy (kJ)
 h_v : Volumetric heat transfer coefficient (W/m².K)
 h_f : Specific enthalpy in a specific temperature (kJ/kg)
 I: Irreversibility rate (kW)
 k : Thermal conductivity (W/m.K)
 m: Mass (kg)
 \dot{m} : Mass flow rate (kg/s)
 p: Pressure (kPa or bar)
 p_d : Power deficit (MW)
 p_g : Generated power (MW)
 p_s : Surplus power (MW)
 Q: Heat transfer rate (kW)
 r: Compression/expansion factor
 \bar{R} : Thermal influential distance (m)
 R: Radius of Cavern (m)
 s: Specific entropy (kJ/kg.K)
 t: Time step (min)
 T: Temperature (°C or K)
 U: Overall heat transfer coefficient (W/m².K)
 V: Volume (m³)
 w: Specific work (kJ/kg)
 W: Work Rate (kW)

Greek symbols

Ψ : Exergy (kJ)
 μ : Thermal capacity ratio
 η : Energy efficiency
 η_{II} : Exergy efficiency
 ψ : Specific exergy (kJ/kg)
 ρ : Density (kg/m³)
 ϵ : Heat exchanger effectiveness factor
 ϵ : Porosity
 δ : Thickness (m)
 €: Euro currency

Subscriptions

a: air
 c: Compressor
 e: External
 en: Energy
 el: Electricity
 ha: Heating air
 i: Internal
 ins: Insulation
 l: Loss
 o: Dead state
 r: Rocks
 tes: Thermal energy storage
 t: Turbine
 w: Water